Coherent energy exchange between components of a vector soliton in fiber lasers

H. Zhang[1], D. Y. Tang[1,*], L. M. Zhao[1], and N. Xiang[2]

1 School of Electrical and Electronic Engineering, Nanyang Technological University, Singapore,639798
2 Center for Optoelectronics, Department of Electrical and Computer Engineering, National University of Singapore, Singapore, 117576
edytang@ntu.edu.sg

Abstract: We report on the experimental evidence of four wave mixing (FWM) between the two polarization components of a vector soliton formed in a passively mode-locked fiber laser. Extra spectral sidebands with out-of-phase intensity variation between the polarization resolved soliton spectra was firstly observed, which was identified to be caused by the energy exchange between the two soliton polarization components. Other features of the FWM spectral sidebands and the soliton internal FWM were also experimentally investigated and numerically confirmed.

OCIS codes: 060.4370 (Nonlinear optics, fibers); 060.5530 (Pulse propagation and temporal solitons); 140.3510 (Lasers, fiber).

References and links

1. O. G. Okhotnikov, T. Jouhti, J. Konttinen, S. Karirnne, and M. Pessa, "1.5-μm monolithic GaInNAs semiconductor saturable-absorber mode locking of an erbium fiber laser," Opt. Lett. **28,** 364-366 (2003).
2. M. Jiang, G. Sucha, M. E. Fermann, J. Jimenez, D. Harter, M. Dagenais, S. Fox, and Y. Hu, "Nonlinearly limited saturable-absorber mode-locking of an erbium fiber laser," Opt. Lett. **24,** 1074-1076 (1999).
3. D. N. Christodoulides and R. I. Joseph, "Vector solitons in birefringent nonlinear dispersive media," Opt. Lett. **13,** 53-55 (1988).
4. B. C. Collings, S. T. Cundiff, N. N. Akhmediev, J. M. Soto-Crespo, K. Bergman, and W. H. Knox, "Polarization-locked temporal vector solitons in a fiber laser: experiment," J. Opt. Soc. Am. B **17,** 354-365 (2000).
5. S. T. Cundiff, B. C. Collings, N. N. Akhmediev, J. M. Soto-Crespo, K. Bergman, and W. H. Knox, "Observation of Polarization-Locked Vector Solitons in an Optical Fiber, "Phys. Rev. Lett. **82,** 3988-3991 (1999).
6. C. R. Menyuk, "Nonlinear Pulse-Propagation in Birefringent Optical Fibers," IEEE J. Quantum Electron. **QE-23,** 174-176 (1987).
7. B. C. Collings, S. T. Cundiff, N. N. Akhmediev, J. M. Soto-Crespo, K. Bergman, and W. H. Knox, "Polarization-locked temporal vector solitons in a fiber laser: theory," J. Opt. Soc. Am. B **17,** 366-372 (2000).
8. S. T. Cundiff, B. C. Collings, and W. H. Knox, "Polarization locking in an isotropic, mode locked soliton Er/Yb fiber laser," Opt. Express **1,** 12-21 (1997).
9. D. Y. Tang, L. M. Zhao, B. Zhao, and A. Q. Liu, "Mechanism of multisoliton formation and soliton energy quantization in passively mode-locked fiber lasers," Phys. Rev. A, **72**, 043816 (2005).
10. N. N. Akhmediev, A. Ankiewicz, M. J. Lederer, and B. Luther-Davies, "Ultrashort pulses generated by mode-locked lasers with either a slow or a fast saturable-absorber response," Opt. Lett. **23,** 280-282 (1998).

1. Introduction

Passive mode-locking of erbium-doped fiber lasers with a semiconductor saturable absorber mirror (SESAM) has been extensively investigated [1, 2]. In contrast to the nonlinear polarization rotation mode-locking, mode-locking incorporating a SESAM does not require any polarization element inside the laser cavity, thereby under suitable condition of the cavity birefringence, vector solitons could be formed in the lasers [3]. Recently, it was reported that even the polarization-locked vector solitons (PLVSs) could be formed in the mode-locked

#96321 - $15.00 USD Received 20 May 2008; revised 25 Jun 2008; accepted 25 Jun 2008; published 6 Aug 2008

fiber lasers [4, 5]. Formation of a PLVS requires not only that the group velocities of the two orthogonal polarization components of a vector soliton are locked but also that their phase velocities are also locked. It is well known that through the self-phase modulation (SPM) and cross-phase modulation (XPM) between the two polarization-modes of a fiber, the group velocity locked vector solitons (GVLVSs) could be formed [6]. Although it was also pointed out that the four-wave-mixing (also called coherent energy exchange) coupling between the polarization components of a vector soliton could have contributed to the formation of the PLVSs [5, 7], so far neither experimental nor theoretical evidence on the soliton internal FWM has been shown. In this Letter we report on the experimental observation of FWM between the two orthogonal polarization components of a vector soliton formed in a fiber laser passively mode locked with a SESAM. A new type of spectral sidebands was first experimentally observed on the polarization resolved soliton spectra of the PLVSs of the fiber lasers. The new spectral sidebands are characterized by that their positions on the soliton spectrum vary with the strength of the linear cavity birefringence, and while on one vector soliton polarization component the sideband appears as a spectral peak, then on the orthogonal polarization component it is a spectral dip, indicating the energy exchange between the two orthogonal polarization components of the vector solitons. Numerically we confirmed that the formation of the new type of spectral sidebands was formed by the FWM between the two polarization components of the vector solitons.

2. Experimental setup

The fiber laser is illustrated in Fig.1. It has a ring cavity consisting of a piece of 4.6 m Erbium-doped fiber (EDF) with group velocity dispersion parameter of 10 ps/km/nm and a total length of 5.4 m standard single mode fiber (SMF) with group velocity dispersion parameter of 18 ps/km/nm. The cavity has a length of $4.6_{EDF}+5.4_{SMF}=10$m. Note that within one cavity round-trip the signal propagates twice in the SMF between the circulator and the SESAM. A circulator is used to force the unidirectional operation of the ring and simultaneously to incorporate the SESAM in the cavity. An intra cavity polarization controller is used to change the cavity's linear birefringence. The laser is pumped by a high power Fiber Raman Laser source (BWC-FL-1480-1) of wavelength 1480 nm. A 10% fiber coupler is used to output the signals. The laser operation is monitored with an optical spectrum analyzer (Ando AQ-6315B), a 26.5 GHz RF spectrum analyzer (Agilent E4407BESA-E SERIES) and a 350 MHz oscilloscope (Agilent 54641A) together with a 5 GHz photodetector. A commercial autocorrelator (Femtochrome FR-103MN) is used to measure the pulse width of the soliton pulses. The SESAM used is made based on a GalnNAs quantum well. The SESAM has a saturable absorption modulation depth of 5%, a saturation fluence of 90 μJ/cm^2 and 10 ps relaxation time. The central absorption wavelength of the SESAM is at 1550nm.

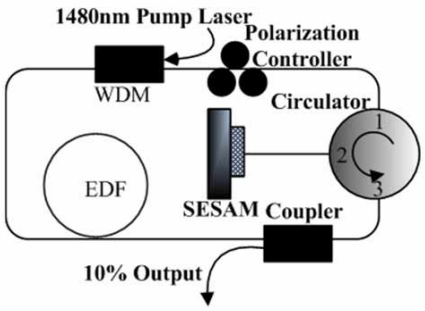

Fig. 1. Schematic of the fiber laser. SESAM: semiconductor saturable absorber mirror; PC: polarization controller; WDM: wavelength-division multiplexer; EDF: erbium-doped fiber.

#96321 - $15.00 USD Received 20 May 2008; revised 25 Jun 2008; accepted 25 Jun 2008; published 6 Aug 2008

3. Experimental results

Experimentally, it was noticed that after mode-locking multiple mode locked pulses were always initially formed in the cavity. Depending on the net cavity birefringence, they were either the GVLVSs, characterized by the rotation of soliton polarization state along the cavity, or the PLVSs, characterized by the fixed polarization at the laser output. With multiple vector solitons in cavity, as a result of mutual soliton interaction complicated relative soliton movement or vector soliton bunches with random fixed soliton separations were observed. To exclude the complications caused by soliton interactions, we have always reduced the number of solitons in cavity through carefully decreasing pump power so that only one or a few widely separated solitons exist in cavity.

Figure 2 shows typical measured optical spectra of the PLVSs of the laser. The soliton feature of the mode-locked pulses is confirmed by the existence of soliton sidebands. However, apart from the existence of the conventional Kelly soliton sidebands, on the vector soliton spectrum there are also extra sets of spectral sidebands. Experimentally it was noticed that different from the Kelly sidebands whose positions are almost independent of the laser operation conditions, such as the pump strength and polarization controller orientation change (linear cavity birefringence change), the positions of the new spectral sidebands varied sensitively with the linear cavity birefringence. We note that Cundiff et al have reported a new type of spectral sidebands on the GVLVS spectrum and interpreted their formation as caused by the vector soliton polarization evolution in the cavity [8]. However, in our experiment the sidebands were observed on the PLVSs, whose polarization remains unchanged as they propagate along the laser cavity.

To determine the physical origin of the extra sideband formation, we then conducted polarization resolved measurement of the vector soliton spectrum. To this end the laser output was first passed through a rotatable external cavity linear polarizer. To separate the two orthogonal polarization components of a vector soliton, we always first located the orientation of the polarizer to the maximum soliton transmission, which sets the long axis of an elliptically polarized vector soliton; we then rotated the polarizer by 90 degree to determine the soliton polarization component along the short axis of the polarization ellipse. Through separating the two orthogonal polarization components of the vector solitons, it turned out that the formation of the extra spectral sidebands was due to the coherent energy exchange between the two soliton polarization components. As can be clearly seen from the polarization resolved spectra, at the positions of extra spectral sidebands, while the spectral intensity of one soliton polarization component has a spectral peak, the orthogonal polarization component then has a spectral dip, indicting coherent energy exchange between them. We note that the energy flow between the two polarization components is not necessarily from the strong one to the weak one. Energy flow from the weak component to the strong component was also observed. In addition, it is to see from the polarization resolved spectra that the extra sidebands are symmetric with respect to the soliton peak frequency and at different wavelength positions the peak-dip can also alternate, suggesting that the energy exchange is the relative phase of the coupled components dependent. Fig. 2 (a) and (b) were obtained from the same laser but under different intra cavity polarization controller orientations. Obviously, the positions of the extra sidebands are the cavity birefringence dependent. Moreover, we observe vector solitons whose polarizations are not locked but rotating. However, their polarization resolved spectra only show one kind of extra spectral sideband which is caused by FWM as well. It thus indicates that FWM spectral sideband is another kind of sideband whose generation mechanism is different from polarization spectral sideband observed by Cundiff et al [8].

#96321 - $15.00 USD Received 20 May 2008; revised 25 Jun 2008; accepted 25 Jun 2008; published 6 Aug 2008

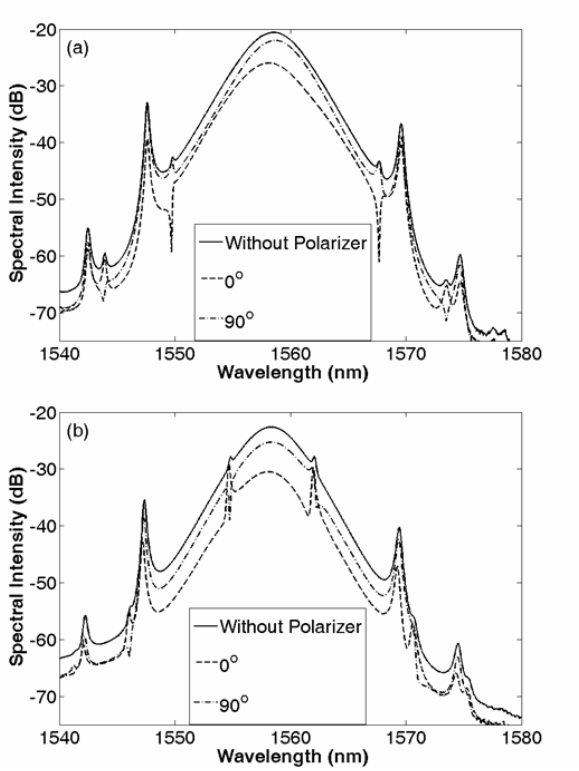

Fig. 2. Optical spectra of the phase locked vector solitons of the laser measured without passing and passing through a polarizer: (a) and (b) were measured under different linear cavity birefringence.

4. Numerical simulations

To verify our experimental observations and determine the extra sideband formation mechanism, we further numerically simulated the effects of the FWM between the two polarization-components of a vector soliton formed in the laser. We used a round-trip model as described in [9] for the simulations. Briefly, we used the following coupled extended Ginzburg-Landau equations to describe the pulse propagation in the weakly birefringent fibers:

$$\begin{cases} \dfrac{\partial u}{\partial z} = i\beta u - \delta \dfrac{\partial u}{\partial t} - \dfrac{ik''}{2}\dfrac{\partial^2 u}{\partial t^2} + \dfrac{ik'''}{6}\dfrac{\partial^3 u}{\partial t^3} + i\gamma\left(|u|^2 + \dfrac{2}{3}|v|^2\right)u + \dfrac{i\gamma}{3}v^2u^* + \dfrac{g}{2}u + \dfrac{g}{2\Omega_g^2}\dfrac{\partial^2 u}{\partial t^2} \\ \dfrac{\partial v}{\partial z} = -i\beta v + \delta \dfrac{\partial v}{\partial t} - \dfrac{ik''}{2}\dfrac{\partial^2 v}{\partial t^2} + \dfrac{ik'''}{6}\dfrac{\partial^3 v}{\partial t^3} + i\gamma\left(|v|^2 + \dfrac{2}{3}|u|^2\right)v + \dfrac{i\gamma}{3}u^2v^* + \dfrac{g}{2}v + \dfrac{g}{2\Omega_g^2}\dfrac{\partial^2 v}{\partial t^2} \end{cases} \quad (1)$$

Where, u and v are the normalized envelopes of the optical pulses along the two orthogonal polarized modes of the optical fiber. $2\beta = 2\pi\Delta n/\lambda$ is the wave-number difference between the two modes and $L_b = \lambda/\Delta n$ is the beat length. $2\delta = 2\beta\lambda/2\pi c$ is the inverse group velocity difference. k'' is the second order dispersion coefficient; k''' is the third order dispersion coefficient and γ represents the nonlinearity of the fiber. g is the saturable gain coefficient of the fiber and Ω_g is the bandwidth of the laser gain. For undoped fibers g=0; for erbium doped fiber, we considered its gain saturation as

#96321 - $15.00 USD Received 20 May 2008; revised 25 Jun 2008; accepted 25 Jun 2008; published 6 Aug 2008

$$g = G\exp[-\frac{\int(|u|^2 + |v|^2)dt}{P_{sat}}] \tag{2}$$

Where G is the small signal gain coefficient and P_{sat} is the normalized saturation energy.

The saturable absorption of the SESAM is described by the rate equation [10]:

$$\frac{\partial l_s}{\partial t} = -\frac{l_s - l_0}{T_{rec}} - \frac{|u|^2 + |v|^2}{E_{sat}} l_s \tag{3}$$

Where T_{rec} is the absorption recovery time, l_0 is the initial absorption of the absorber, and E_{sat} is the absorber saturation energy. To make the simulation possibly close to the experimental situation, we used the following parameters: γ=3 $W^{-1}km^{-1}$, Ω_g =24nm, P_{sat}=100 pJ, k''_{SMF}= -23 ps^2/km, k''_{EDF}= -13 ps^2/km, k'''= -0.13 ps^3/km, E_{sat}=1pJ, l_0=0.15, and T_{rec} = 6 ps, Cavity length L= 10 m.

Figure 3 shows the results obtained. Extra spectral sidebands appeared clearly on the vector soliton spectrum of the laser. In particular, the extra sidebands of the orthogonal soliton polarization components exhibited out-of-phase intensity variations. To verify that the extra spectral sidebands were caused by the FWM between the orthogonal soliton polarization components, we deliberately removed the coherent coupling terms in our simulations. Without the FWM terms no extra spectral sidebands were observed. Numerically, it was also noticed that the appearance of the extra sidebands is related to the small linear cavity birefringence. When the linear cavity birefringence is set zero, although strong energy exchange exists between the two polarization components, no extra sidebands were observed, instead the overall soliton spectrum exhibits “peak-dip” alternation as the soliton propagates in cavity. Moreover, numerical simulations have also exhibited the dependence of extra sideband positions with the linear cavity birefringence.

The numerical simulations well reproduced the extra spectral sidebands and confirmed that their appearance is indeed caused by the FWM between the orthogonal soliton components. Based on the numerical model we further investigated the FWM interaction between the soliton polarization components and its impact on the vector soliton. Numerically it was observed that as a result of the weak linear cavity birefringence, FWM between the two vector soliton components occurred. The FWM caused an antiphase type of periodic pulse intensity variation between the two orthogonally polarized soliton components, and the stronger the linear cavity birefringence the weaker the periodic pulse intensity variation. However, independent of the cavity birefringence the pulse intensity of the vector soliton always remained constant. The observed features of the vector solitons could be easily understood. Due to small linear cavity birefringence, coherent coupling between the two polarization components of a vector soliton can no longer be neglected. Its existence causes coherent energy exchange between the two orthogonal soliton polarization components. Nevertheless, as far as the linear cavity birefringence is not zero, energy exchange does not occur at whole soliton spectrum, but only at certain wavelengths where the phase matching condition is fulfilled under the aid of the laser cavity, which then leads to the formation of the discrete extra spectral sidebands. However, as the FWM is a parametric process and occurs between the internal components of a vector soliton, its appearance only causes an antiphase periodic intensity variation between the coupled soliton components but not the intensity of the vector soliton.

#96321 - $15.00 USD Received 20 May 2008; revised 25 Jun 2008; accepted 25 Jun 2008; published 6 Aug 2008

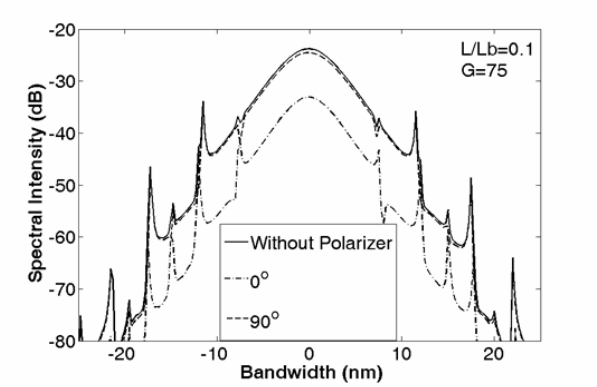

Fig. 3. Numerically calculated optical spectra of the vector solitons formed in fiber ring lasers.

5. Conclusion

In conclusion, we have experimentally observed a novel new type of spectral sideband generation on the soliton spectra of the phase locked vector solitons in a passively mode-locked fiber ring laser. Polarization resolved study on the soliton spectrum revealed that the new sidebands were caused by the coherence energy exchange between the two orthogonal polarization components of the vector solitons. Numerical simulations have confirmed our experimental observation.

Acknowledgement

This project is supported by the National Research Foundation Singapore under the contract NRF-G-CRP 2007-01.

#96321 - $15.00 USD Received 20 May 2008; revised 25 Jun 2008; accepted 25 Jun 2008; published 6 Aug 2008